

## **Influence of CdS Layer on Texture Characteristics of CdTe Films Grown by CSS Combined with Substrate Rotation**

V. Vazquez-Vera, A. Duarte-Moller, R. Medina-Esquivel, R. Castro-rodríguez, I. Pérez Quintana, J. Mendez-Gamboa, E. Chan y Díaz.

### **Abstract**

Influence of the thickness of CdS layer on the texture characteristics (morphology and crystalline structure) of the photovoltaic active layer CdS/CdTe was studied. CdS and CdTe films were grown by Close Space Sublimation technique combined with Substrate Rotation (CSSSR). In order to growth the CdTe films, three glass substrates with previously deposited CdS thin film with thicknesses of 106.3, 125.1 and 221.0 nm respectively were used. The conditions of CdTe films deposition were, vacuum pressure of  $1 \times 10^{-6}$  mTorr, sublimation source temperature 650 oC, substrate temperature 280 oC, source-substrate distance 5.0 mm, substrate rotation 1025 rpm and time deposition 10 min. The CdTe films obtained were with uniform thickness and dimensions of  $\sim 4.73 \mu\text{m}$  and compacted grain with sizes of 112.5, 108.2 and 140.3 nm respectively. The samples shown high quality crystalline with a preferential orientation in the plane (111), and the CdTe unit cell volume was less than the standard pattern as a consequence of lattice contraction due at the formation of Cd vacancies confirmed by EDAX technique. Keyword-Component: closed space sublimation, flash deposition technique, CdTe thin films, physical properties.

### **Introduction**

To solar cells CdS/CdTe, a reduction in the thickness of the active layer photovoltaic, is one of the most important requirements from the viewpoint of cost

reduction as well as the influence of Cd toxicity. For the improvement in the development of photovoltaic efficiency, the influence of the CdS layer, especially the thickness  $d_{CdS}$ , should be investigated because high efficiencies ~16% have been found with  $d_{CdS} \sim 100$  nm for solar cells CdS/CdTe with  $d_{CdTe} > 100$  nm for solar cells CdS/CdTe with  $d_{CdTe} > 3 \mu\text{m}$  [1-2]. It is well known that CdS layer acts as a window layer which is related to the spectral response in regions of low wavelength and plays a crucial role in the crystallinity of CdTe layer and the formation of the ternary compound  $\text{CdS}_x\text{Te}_{1-x}$  between layers CdS/CdTe. Work done on this subject have demonstrated the optimization of critical parameters of a solar cell CdS/CdTe as the photocurrent density, fill factor, open circuit voltage and the efficiency of the cell as a function of  $d_{CdS}$  [3], also has been reported the critical value  $x$  and the gap of the ternary  $\text{CdTe}_{1-x}\text{S}_x$  as function of  $d_{CdS}$ .

On the other hand, thin films of CdS and CdTe have been grown with different deposition techniques to achieve high efficiencies in CdS/CdTe cells [4-7]. The deposition techniques are basically for CdS thin films, chemical bath deposition (CBD), sputtering deposition, closed space sublimation (CSS) and chemical vapor deposition (CVD).

For the deposition of CdTe films common technique used is CSS. In this work, we report the morphological and structural properties of CdTe films with thicknesses of  $\sim 4.73 \mu\text{m}$  deposited by CSS technique modified with Substrate Rotation (CSSSR) on CdS thin films with different thicknesses deposited earlier by CSSSR [8].

## Experimental details

Three glass substrates with a thin layer of CdS with different thicknesses of 106.3, 125.1 and 221.0 nm respectively were used, the experimental details of the CdS growth condition is previously reported [8]. The samples were named C1LA (106.3 nm), C2LA (125.1 nm) and C3LA (221.0 nm). The substrates were washed separately before use with isopropyl alcohol in an ultrasonic bath during 5 min. After this period the substrate was taken out of the beaker, and rinsed with distilled water and dried with compressed inert gas. For the deposition of CdTe films, we used the technique of CSSSR. The experimental setup is shown in Fig. 1. This consists of a graphite container heated by a 300 W halogen lamp OSRAM. The lamp is supported by a stainless steel cylinder, and deposit material (CdTe pressed powder) is placed in the container of graphite.

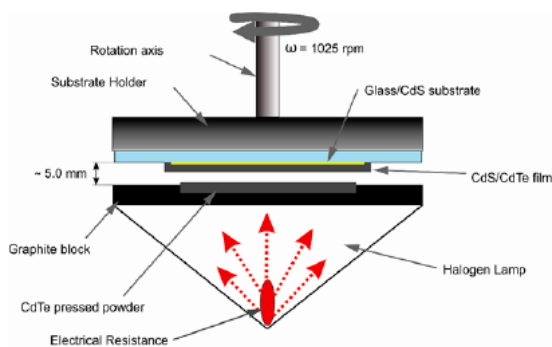


Figure 1. Experimental setup used in the technique of Close Space Sublimation combined with Substrate Rotation.

The substrate is kept at a distance from the edge of the stainless steel cylinder of 5.0 mm and is rotated at 1025 rpm. The experimental setup is placed in a vacuum chamber of  $1 \times 10^{-6} \text{ mTorr}$ . The film growth is facilitated by using a "shutter" glass placed between the substrate and the stainless steel cylinder. The substrate is heated by radiation from the halogen lamp. The cycle of deposition of CdTe film is as follows: the

graphite is heated at 650 °C in 10 min, and by radiation the substrate reaches a temperature of 280 °C in dependence of edge source-substrate distance, then the "shutter" is opened and the CdTe film is obtained. After deposition time of 10 min, the temperature gradually decreases to room temperature.

The thickness ( $d$ ) of the films was measured by a surface profilometer Dekpak-8 Veeco. The crystallographic orientations were studied by X-ray diffraction (XRD) using a Siemens D-5000 Siemens diffractometer with Cu-  $K\alpha$  wavelength monochromatic radiation ( $\lambda = 1.541 \text{ \AA}$ ) at 34 kV and 25 mA. To determine the stoichiometry of the films, EDAX was used in a Scanning Electron Microscope (SEM) Phillips XL30 with a source of electrons of 25 kV. The morphology of the films was analyzed by SEM and atomic force microscopy (AFM) using an Auto-Probe CP from Park Scientific Instruments in the constant force mode with a high-resolution scanner.

## Results and discussion

A schematic representation of the structure CdS/CdTe solar cell can be seen in Fig. 2, this is a view of a cross section. The CdS and CdTe films deposited are squares with dimension of 1.0 inch square.



Figure 2. Schematic representation of the structure CdS/CdTe.

The inverted triangle and positioned on the CdTe film represents the tip of the profilometer that scans a distance  $D$  to the right in order to measuring the thickness of the CdTe film as well as uniformity. Figure 3 shows the experimental results for samples C1LA, C2LA, C3LA respectively.

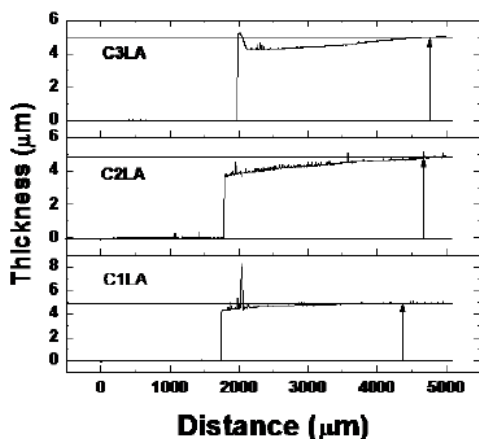


Figure 3. Experimental results of the thickness of the CdTe films for samples C1LA, C2LA, C3LA respectively.

The uniformity profile of the thickness of CdTe for each sample is very noticeable; however, we can see a peak on the edge of the thicknesses of the samples and a slight increase far as distance where starts the uniformity of the CdTe film indicated by the vertical arrow. The C1LA sample shows a better uniformity from the beginning of the edge of the thickness. This can be attributed to the thickness of CdS film, due that is smaller than the other two samples. The peaks observed in each one of the profiles are clusters of CdTe, a likely explanation is due to growth of CdTe in the edge of thickness after that substrate rotation is stopped; although the "shutter" is placed, residual atoms of Cd and Te can be condensed on the edge of the CdTe film and generate clusters. The thickness measurements of the CdTe films were determined

by subtracting the thickness of CdS film. These results are shown in Table I, and the average value was  $\sim 4.73 \mu\text{m}$ , confirming that the thicknesses of the CdTe films are reproducible.

Sample	$d_{\text{measured}} (\mu\text{m})$	$d_{\text{CdS}} (\mu\text{m})$	$d_{\text{CdTe}} (\mu\text{m})$
C1LA	4,896	0,106	4,79
C2LA	4,771	0,125	4,646
C3LA	4,969	0,221	4,748

SEM measurements were made to determine the surface morphology of CdTe films for different amplifications. The images obtained are shown in Fig. 4 and these were taken at the center of each sample.

The images show the impact of the CdS thickness ( $d_{\text{CdS}}$ ) on CdTe film. The image 500x of the sample C1LA shows a surface clean of cluster, uniform and compact in an area of  $250 \mu\text{m} \times 250 \mu\text{m}$ . Images of smaller areas to 5000x and 10000x respectively, show evidence of uniformity in the grains formation. Samples C2LA and C3LA show small rougher surfaces than the first sample, 5000x and 10000x images in both samples show some holes formations between the grains. Although an increased roughness is evident, the grains are very compact in both samples.

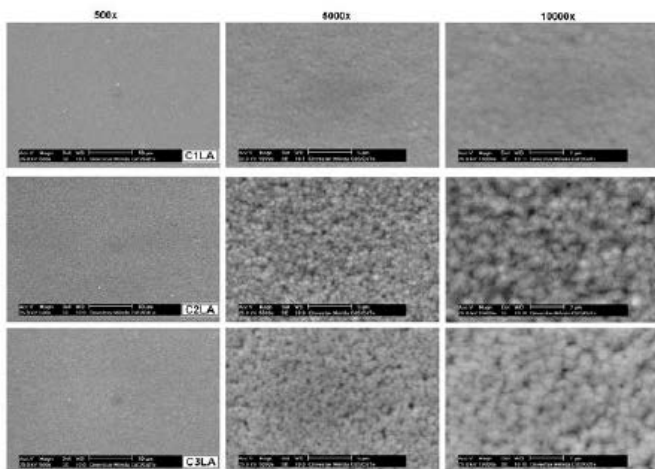


Figure 4. SEM Micrographs of CdTe films for amplifications of 500x, 5000x and 10000x respectively.

Figure 5 shows AFM images of  $2 \times 2 \mu\text{m}^2$  in 2D and 3D for samples C1LA, C2LA and C3LA respectively. We can see different grain sizes but with same forms. In general the surfaces are very smooth and compact; these microstructures are due to crystallization and coalescence processes between grains. This could be explained not only by  $d_{\text{CdS}}$  effect, also by the substrate rotation effect which produces a higher probability of formation of nucleation sites, and then the grains tend to coalesce between them resulting in more uniform and compact grains. Figure 6 shows the profiles between valleys and maximum heights of the grains with respect to preferred distance of the samples, it is show the heights between valleys and maximum height for the determination of the root means square (rms) roughness of the samples. Figure 7 shows the characteristic of granular density and the rms of the CdTe films as a function of  $d_{\text{CdS}}$ .

The average of the granular density of the samples was calculated by counting the total number of grains of CdTe in the area of  $2 \times 2 \mu\text{m}^2$  on 2DAFM images and the average values were  $\sim 108$  grains/ $\text{cm}^2$ . However, the sample C1LA showed a major

density. The mean-square roughness is equivalent to the average deviation of the heights. The values were obtained using the program WSxM 3.1 [9], which made the calculation of 2D-AFM images. These values were 34.41, 38.02 and 25.03 nm for samples C1LA, C2LA, and C3LA respectively. The sample C3LA showed less roughness, while samples C1LA and C2LA showed a similar roughness.

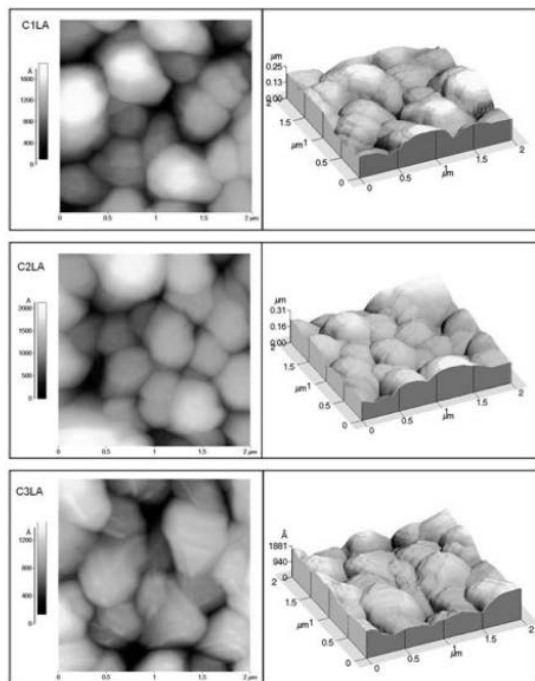


Figure 5. AFM images of  $2 \times 2 \mu\text{m}^2$  in 2D and 3D for C1LA, C2LA and C3LA samples respectively.

Figure 8 shows the X-ray diffraction patterns of the samples C1LA, C2LA and C3LA respectively compared with the standard pattern of CdTe [10]. It is clear that the crystalline structure of the CdTe films was cubic (zincblende) and we can see a clear preferential orientation of the plane (111) parallel to the substrate, which shows a high quality crystalline of the CdTe films.



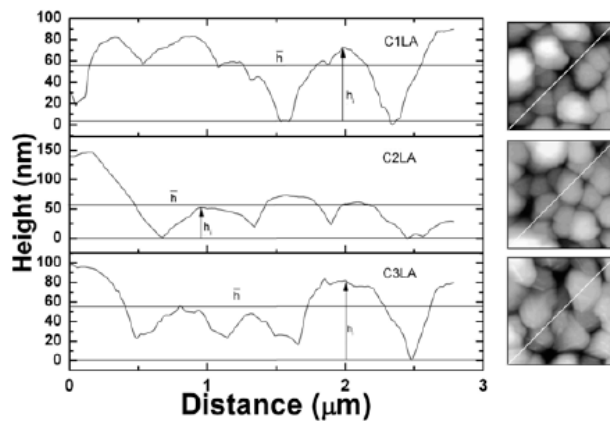


Figure 6. Profiles between valleys and maximum heights of the grains with respect to a preferred distance of the samples

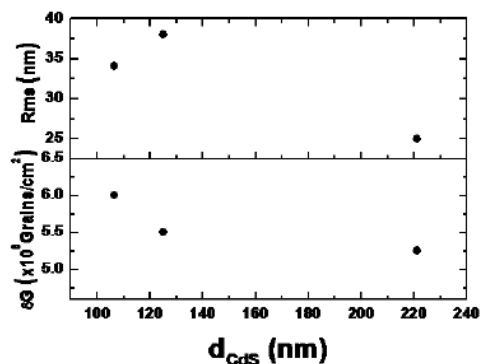


Figure 7. Behavior of granular density and the rms of the CdTe films as a function of thickness CdS film

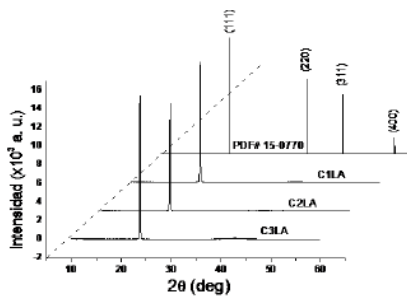


Figure 8. XRD spectra of CdTe films corresponding at samples C1LA, C2LA and C3LA respectively.

Figure 9 shows the behavior of the intensity (111) peak (placed on  $2\theta = 23.80 \pm 0.02^\circ$ ) and grain size as a function of thickness CdS film.

The peak most intensity correspond to sample C3LA. The grain sizes of the films were obtained using the Scherrer formula [11]. These values were 112.5, 108.2 and 140.3 nm for samples C1LA, C2LA, and C3LA respectively, indicating a regular uniformity in the films.

Figure 10 shown behavior of the volume of the unit cell in function of the  $d_{CdS}$ . It is evidences that as the thickness of the CdS film increase, the increase volume on the CdTe, comes closer to the pattern value. This can be also seen in the displacement of the (111) peak with respect to the standard pattern, as showed in the Fig. 11.

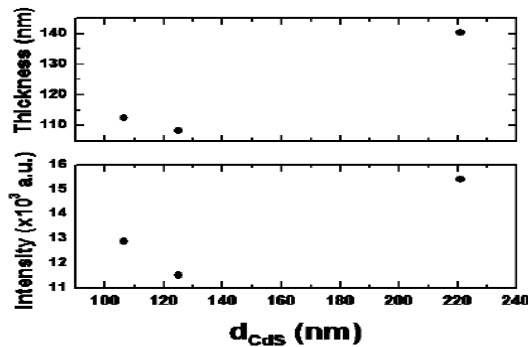


Figure 9. Behavior of the intensity (111) peak and grain size as a function of thickness CdS film.

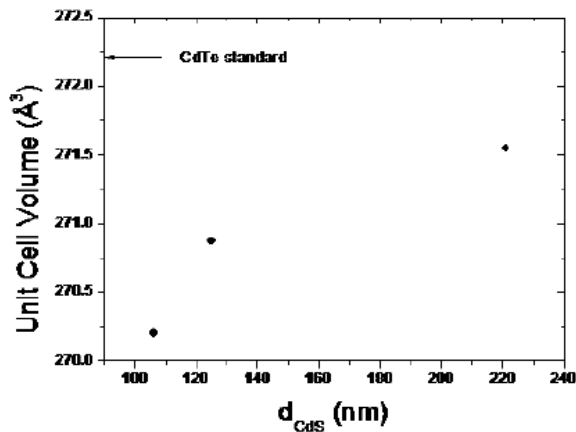


Figure 10. Behavior of the volume of the CdTe unit cell as a function of the thickness CdS films.

This indicates one stress as a consequence of contraction on the CdTe unit cell and then different values of the lattice parameters in comparison with the value reported by the pattern standard of 6.481 Å (JCPDS 2005) were measurements. Those values obtained were 6.465, 6.470 and 6.476 Å for samples C1LA, C2LA, and C3LA respectively.

The volume of the unit cell were 270.2, 270.9 and 271.5 Å<sup>3</sup> for samples C1LA, C2LA, and C3LA respectively in comparison with the reported standard value of 272.22 Å<sup>3</sup>. One explanation of these behaviors is that probably a less thickness of CdS causes a bigger quantity of Cd vacancies than could be present in the unit cell of CdTe. This was confirming from the stoichiometry by EDAX measurements. In the table II these values are indicated to each one of the samples. We can see that the atomic percentage is higher for telluride, that for cadmium and as a consequence the evidence of Cd vacancies.

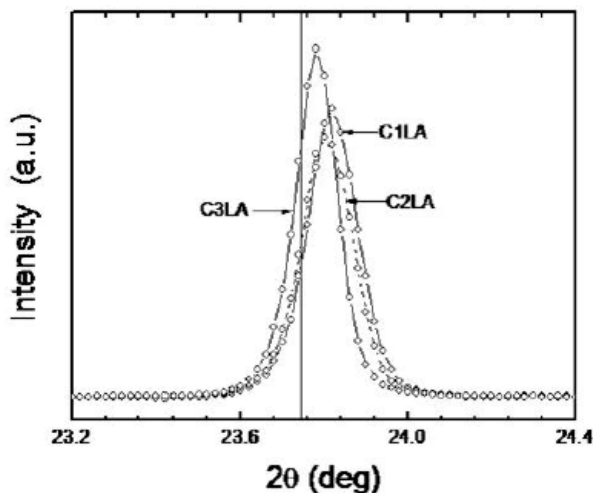


Figure 11. Displacement of the CdTe (111) peak with respect to the standard pattern.

## Conclusions

CdTe films were grown by CSSSR. The CdTe source temperature was 650 °C, and the substrate temperature 280 °C. Three CdS substrates previously deposited with thicknesses of 106.3, 125.1, and 221.0 nm using also CSSSR were used. The CdS substrate rotation was fixed at 1025 rpm. To analyze the influence of the thickness of the CdS layers on the texture characteristics of CdS/CdTe the samples were analyzed by XRD, SEM, EDAX, AFM, and surface profilometer techniques. In profilometer we found that the samples were reproducibility with thickness of the CdTe films of  $4.728 \mu\text{m} \pm 0.074 \mu\text{m}$ . The sample C1LA, show smaller thickness of CdS and present the better uniformity. XRD shows a preferential orientation in the plane (111) for the three samples. It is evident a displacement in the main peak (111) in comparison with the standard pattern, that indicated the lattice parameters decreases, as a consequently the cells present a volume smaller than standard volume. This contraction in the unit cell was corroborated with the concentration ratio Cd/Te taken from EDAX, where we concluded the formation Cd vacancies. The morphology of the films shows that the samples were free of conglomerates due at  $d_{cds}$  and the rotation effect of the substrate. We observed a bigger uniformity and compact grain size in the sample C1LA, in contracts for the samples C2LA and C3LA low ruggedness is observed and some holes among the grains. AFM value of the density grains for each samples were of the order of  $10^8$  grains/cm<sup>2</sup>. Measurements of rms were also obtained by this technique, and it is found that in an area of  $2 \times 2 \mu\text{m}^2$ , the sample C2LA show a major rms, and the sample C3LA the value of rms was smaller.

## **Acknowledgment**

The authors would like to thank Oswaldo Gómez, Mario Herrera, Wilian Cauich, Oscar Ceh and Daniel Aguilar for technical assistance, also to Mrs. Lourdes Pinelo for secretary assistance. This work has been supported under project No. 59996 CONACYT/México. E. Chan y Díaz acknowledges also CONACyT/México for his scholarship in the Advanced Materials Research Center, (CIMAV), from Chihuahua, National Laboratory of Nanotechnology at CIMAV.

## References

- [1] Aramoto T, Kumazawa S, Higuchi H, Arita T, Shibutani S, Nishino T, Nakajima T, M. Tsuji, Hanafusa A, Hibino T, Omura K, Ohyama H, Murozono M (1997). 16.0% Efficient Thin-Film CdS/CdTe Solar Cells. *Jpn. J. Appl. Phys.*, 36: 6304-6305.
- [2] [2] Britt J, Ferekides C (1993). Thin-film CdS/CdTe solar cell with 15.8% efficiency. *Appl. Phys. Lett.*, 62: 2851-2852.
- [3] [3] Nakamura K, Gotoh M, Fujihara T, Toyama T, Okamoto H (2003). Influence of CdS window layer on 2- $\mu$ m thick. CdS/CdTe thin film solar cells. *Solar Energy Materials & Solar Cells*, 75: 185-192.
- [4] [4] Lee J, Yi J, Yang K, Park J, Oh R (2003). Electrical and optical properties of boron doped CdS thin films prepared by chemical bath deposition. *Thin Solid Films*, 431-432: 344-34.
- [5] [5] Castro-Rodríguez R, Oliva A I, Sosa V, Caballero-Briones F, Peña J L (2000). Evidence of pure diffusion process on growth of gold films. *Appl. Surf. Sci.*, 161: 340-346.

[6] [6] Rami M, Benamar E, Fahoume M, Chraibi F, Ennaoui A (1999). Effect of the Cadmium Ion Source on the Structural and Optical Properties of Chemical Bath Deposited CdS Thin Films. *Solid State Sci.*, 1: 179-188.

[7] [7] Bonilla S, Dalchicle E A (1991). Electrochemical deposition and characterization of CdTe polycrystalline thin films. *Thin Solid Films*, 204: 397-403.

[8] [8] Castro-Rodríguez R, Méndez-Gamboa J, Pérez-Quintana I, Medina- Esquivel R (2011). CdS thin films growth by fast evaporation with substrate rotation. *Appl. Surface Sci.*, 257: 9480- 9484.

[9] [9] Horcas I, Fernández R, Gómez-Rodríguez J M, Colchero J, Gómez-Herrero J, Baro A M (2007). WSXM: A software for scanning probe microscopy and a tool for nanotechnology. *Rev. Sci. Instrum.*, 78: 013705.

[10] [10] JCPDS (2005). International Center Diffraction Data, PDF Card No. 15-0770.

[11] [11] Cullity B D (1978). *Elements of X-ray Diffraction*, Addison- Wesley, pp. 87-102.